Scanning gate microscopy of current-annealed single layer graphene

M. R. Connolly,[1,a)] K. L. Chiou,[1] C. G. Smith,[1] D. Anderson,[1] G. A. C. Jones,[1]
A. Lombardo,[2,3] A. Fasoli,[3] and A. C. Ferrari[3]

[1]*Department of Physics, Cavendish Laboratory, University of Cambridge, Cambridge CB3 0HE, United Kingdom*
[2]*Universitá degli Studi di Palermo, Dipartimento di Ingegneria Elettrica, Elettronica e delle Telecomunicazioni, Viale delle Scienze, 90128 Palermo, Italy*
[3]*Department of Engineering, University of Cambridge, Cambridge CB3 OFA, United Kingdom*

We have used scanning gate microscopy to explore the local conductivity of a current-annealed graphene flake. A map of the local neutrality point (NP) after annealing at low current density exhibits micron-sized inhomogeneities. Broadening of the local e-h transition is also correlated with the inhomogeneity of the NP. Annealing at higher current density reduces the NP inhomogeneity, but we still observe some asymmetry in the e-h conduction. We attribute this to a hole-doped domain close to one of the metal contacts combined with underlying striations in the local NP. © *2010 American Institute of Physics*. [doi:10.1063/1.3327829]

Graphene exhibits a wealth of properties relevant to a wide range of applications and fundamental research.[1] For graphene to meet expectations and complement silicon in future nanoelectronics it will be necessary to obtain precise and consistent control over its nanoscale electronic properties. Promising steps in this direction have been made using a combination of chemical functionalization and geometrical confinement.[2–6] Developing techniques for analyzing and controlling the effect of these processes is thus at the forefront of graphene research. Scanning probes in particular have provided valuable insights into the substrate's influence on nanometer-scale topographic and potential fluctuations,[7–10] while photocurrent[11,12] and Raman[13–16] microscopy have been used to probe mesoscopic variations in doping from charged surface impurities and invasive metal contacts. The presence of charged impurities manifests in the electrical transport as a shift in the charge neutrality point (NP) (see Ref. 17) but the effect on the mobility and minimum conductivity at the NP is still debated.[18,19] Mesoscopic (micron-sized) inhomogeneities in the impurity density also contribute to the random variations observed in the transport properties of as-prepared two terminal devices.[20] Annealing in an inert atmosphere and degassing reduces the NP shift and inhomogeneity,[21,22] but unless a final cleaning step is performed *in situ* the improvement is limited due to the re-adsorption of atmospheric gases and water vapor.[22] Current annealing has been used for *in situ* removal of adsorbates,[23,24] in many cases resulting in an electron-hole conduction asymmetry.[2,23,25] Here, we use scanning gate microscopy (SGM) (see Ref. 26) to explore the local conductivity of a current-annealed graphene monolayer and show that persistent inhomogeneities in the remanent impurity density contribute to the anomolous e-h conduction.

We investigate a graphene flake ($\sim 8 \times 8$ μm^2) mechanically exfoliated from natural graphite onto a n$^+$-Si substrate capped with 300 nm SiO$_2$. Optical microscopy[27] and Raman spectroscopy[28] were used to locate the flake and confirm that it was a monolayer. Two 50 nm thick Au contacts

were patterned using e-beam lithography and lift-off processing [see inset of Fig. 1(a).] The sample was annealed at 200 °C in N$_2$/H$_2$ (5%) to remove resist residue and mounted to the head of our SGM system. The microscope chamber was evacuated to 10^{-5} mbar and further cleaning was performed *in situ* by driving $J \approx 5 \times 10^8$ A/cm^2 through the device and monitoring the shift in the neutrality point voltage (V_{NP}).[23] The two terminal resistance R as a function of voltage V_{BG} applied to the Si back-gate reveals ≈ 3 V reductions in V_{NP} every 10 minutes [Fig. 1(a).] The initial $V_{NP} \approx 20$ V is most likely due to hole-doping from adsorbed H$_2$O.

Using $n = \alpha(V_{BG} - V_{NP})$ ($\alpha = 7.2 \times 10^{10}$ cm^{-2}) (Ref. 17) to estimate the carrier density, we obtain a mobility of ≈ 8000 cm^2 V^{-1} s^{-1} at $n = 2 \times 10^{11}$ cm^{-2}. The final cleaning current was applied for 9 hours, resulting in $V_{NP} \approx 15$ V and a shoulder appearing around $V_{BG} = 6$ V [red (dotted) curve, Fig. 1(a).] The latter is characteristic of flakes divided into regions with different carrier density, either by chemical doping,[21,29] or invasive metal contacts.[20] The suppression of R is also typical of flakes with a mesoscopic NP inhomogeneity.[20,21]

We operate our SGM in non-contact mode [see Fig. 1(b)] with an average tip-surface separation of ~ 5 nm. To benefit from the high signal-to-noise ratio achievable using lock-in detection, we modulate the voltage V_T on the tip
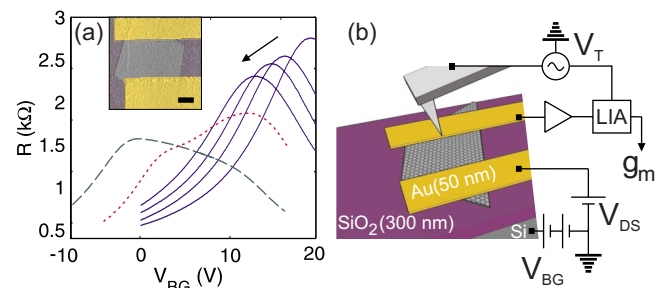
FIG. 1. (Color online) (a) $R(V_{BG})$ measured at 10 min. intervals (blue, solid) and after 9 h (red, dotted) of current annealing at $J \approx 5 \times 10^8$ A/cm^2 (arrow indicates the direction of peak position shift.) After 10 min at $J \approx 1 \times 10^9$ A/cm^2 (green, dashed.) Inset: False-color atomic force micrograph of the sample (scale bar is 2 μm.) (b) Schematic of the SGM setup.

a)Electronic mail: mrc61@cam.ac.uk.

96, 113501-1
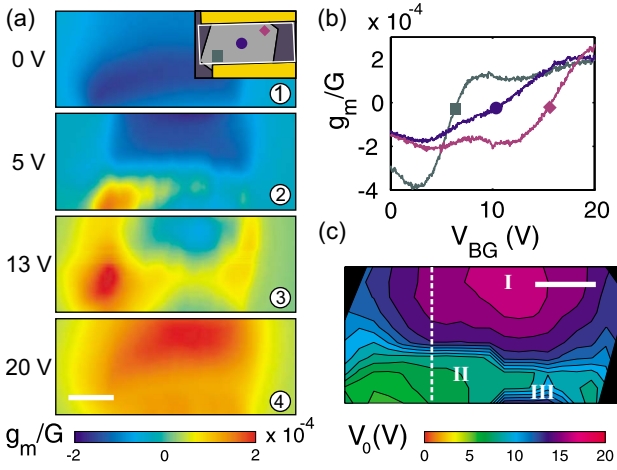
FIG. 2. (Color online) (a) Series of raw $g_m(x,y)$ images captured at different V_{BG}. Inset: device schematic (white outline indicates scan area.) (b) Normalized $g_m(V_{BG})$ measured with the tip at the locations marked in the inset of (a). (c) Contour plot of V_0 with the flake in the state corresponding to the red (dotted) $R(V_{BG})$ sweep in Fig. 1(a). Scale bars are 2 μm.

FIG. 3. (Color online) (a) $\sigma_L(V_{BG})$ reconstructed by integrating the $g_m(V_{BG})$ sweeps in Fig. 2(b). Each curve has been vertically offset such that $\sigma_L(V_0)=0$. (b) Correlation plots between ΔV_{BG} and ΔV_0. Dashed line indicates the linear trend.

(NanoWorld ARROW-NCPt) at low frequency (typically 3 V@1 kHz) and detect the modulation of I_{DS} (~ 250 μA) using a lock-in amplifier. We quantify the demodulated component δI_{DS} by the local transconductance $g_m = \partial I_{DS}/\partial V_T$ (~ 0.2 μA/V) normalized to the bulk conductance $G(V_{BG})$.[26]

Figure 2(a) shows a series of raw $g_m(x,y)$ images of the device captured at different back-gate voltages. When $V_{BG} < 6$ V, G is suppressed ($g_m < 0$) over the entire flake (image 1.) With increasing V_{BG}, a disordered domain spanning the width of the flake changes sign (image 2) and expands along the edges toward each contact (image 3.) Eventually G is uniformly enhanced ($g_m > 0$) when $V_{BG} > 16$ V (image 4.) Figure 2(b) shows typical $g_m(V_{BG})$ measured with the tip in the regions marked in the inset of Fig. 2(a). While the form of $g_m(V_{BG})$ is similar in each region, the crossover back-gate voltage when g_m changes sign [$V_0 = V_{BG}(g_m=0)$] varies with position between 6 V $< V_{BG} <$ 16 V, giving rise to the contrast observed in Fig. 2(a).

To understand the basic form of the measured $g_m(V_{BG})$, we relate the conductivity σ_L of the $\approx (50$ nm$)^2$ area perturbed by the tip[10] to a local carrier density $\sigma_L(x,y) \propto |\alpha V_{BG} + \beta V_T + \bar{n}| e \mu$, where β ($\approx 5 \times 10^{11}$ cm^{-2}) (Ref. 10) is the capacitive coupling between the tip and graphene, and $\bar{n}$ is the local impurity-induced carrier density.[19,30,31] Neglecting quantum contributions to σ_L, we expect g_m to reflect the variation of $\partial \sigma_L(x,y)/\partial V_T \propto \mu$ [if $\mu \neq \mu(n)$,] implying that the carriers in the negative and positive $g_m(x,y)$ domains in Fig. 2(a) are holes ($\mu_h < 0$) and electrons ($\mu_e > 0$). Furthermore, since μ changes sign at the local NP when $V_{BG} = V_0 \approx -\bar{n}(x,y)/\alpha$ [$\langle V_T \rangle = 0$,] it follows that V_0 is a measure of $\bar{n}$, which can be empirically related to the impurity density n_i.[19]

We explore $\bar{n}(x,y)$ by measuring $g_m(V_{BG})$ with the tip positioned over a grid with 300 nm pitch and constructing the map of $V_0(x,y)$ shown in Fig. 2(c). A region (II) with $V_0 = 6$ V ($\bar{n} \approx 4 \times 10^{11}$ cm^{-2}) runs across the flake parallel to the contacts, asymmetrically flanked by semi-circular regions (I and III) close to the contacts, where $V_0 = 15$ V ($\bar{n} \approx 10^{12}$ cm^{-2}). We believe that this remanent impurity density map reflects the temperature distribution generated by
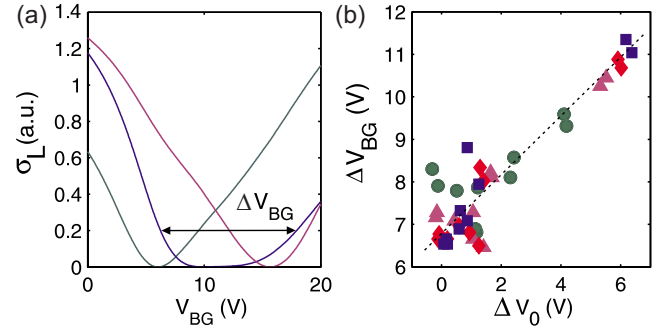
ohmic heating during current annealing. Here the higher temperatures (lower V_0) are reached at the center and edges of the flake, while the lower temperature (higher V_0) regions seem to extend outward from the middle of the metal-graphene interface, possibly due to heat sinking.[32] A similar temperature distribution was inferred from previous scanning probe[23] and Raman[32] microscopy measurements, although here the asymmetry either side of the higher temperature region is more pronounced. The two values of V_0 also coincide with the positions of the shoulder and the maximum of the bulk $R(V_{BG})$, confirming that these features originate from the mesoscopic NP inhomogeneity.

Figure 3(a) shows plots of the local conductivity $\sigma_L(V_{BG})$ reconstructed by numerically integrating the $g_m(V_{BG})$ sweeps in Fig. 2(b). Within the framework of Ref. 30, the width of the minimum conductivity plateau ΔV_{BG} at the NP is expected to increase with $\bar{n}$.[19,30] While we did not observe this direct relationship, Fig. 3(b) reveals a linear correlation between ΔV_{BG} and ΔV_0, the change in V_0 along linescans in the vicinity of the dashed line in Fig. 2(c). (We extract ΔV_{BG} for each curve by subtracting the back-gate voltages where $\sigma_L = 0.2$.) Broadening of $\sigma_L(V_{BG})$ is thus most pronounced when the tip gates both electron and hole domains, in the same way that ΔV_{BG} in homogeneous flakes is broadened by e-h puddles at low carrier density.[30]

To assess the inhomogeneity remaining when $V_{NP} \approx 0$ V, we annealed the flake at $J \approx 10^9$ A/cm^2 and repeated the measurement of $V_0(x,y)$. The result is shown in Fig. 4(a) and the corresponding $R(V_{BG})$ sweep by the green (dashed) curve in Fig. 1(a). In line with the previous analysis, the single peak in $R(V_{BG})$ coincides with the average value of $V_0 \approx 2$ V ($\bar{n} \approx 10^{11}$ cm^{-2}), and the greater homogeneity is reflected by the absence of the shoulder. However, upon close inspection we observe a region around the top contact
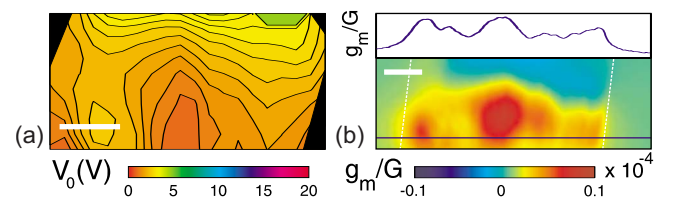
FIG. 4. (Color online) (a) Contour plot of V_0 with the flake in the state corresponding to the green (dashed) $R(V_{BG})$ curve in Fig. 1(a). (b) Raw $g_m(x,y)$ image (12×5 μm^2) ($V_{BG}=3$ V) together with a line profile of g_m taken along the blue line in the image. Scale bars are 2 μm.

with $V_0 = 8-10$ V. The doping in this region, which persisted even after annealing with $J > 10^9$ A/cm^2, is responsible for the kink in $R(V_{BG})$ at $V_{BG} = 10$ V. Superimposed on this micron-sized inhomogeneity we also observe striations in g_m running between the contacts with lateral period of ≈ 100 nm [Fig. 4(b).] These modulations could be caused by enhanced heating from resistive hotspots in the disordered *pn* junctions formed close to the metal-graphene interface,[20] or electromigration from the contacts.[23] We estimate they reflect an impurity density fluctuation of $\Delta\bar{n} \sim 10^9$ cm^{-2}, which may impose an intrinsic limit to the homogeneity achievable when current annealing supported flakes.

In conclusion, SGM is a powerful method for characterizing the local conductivity of inhomogeneously doped graphene. The local NP reflects the temperature distribution generated by ohmic heating and also exhibits finer linearly correlated inhomogeneities. Both types of inhomogeneity are likely to contribute to the e-h conduction asymmetry observed in current-annealed graphene flakes.

[1] A. K. Geim and K. S. Novoselov, Nature Mater. **6**, 183 (2007).
[2] X. Wang, X. Li, L. Zhang, Y. Yoon, P. K. Weber, H. Wang, and H. Dai, Science **324**, 768 (2009).
[3] M. Y. Han, B. Ozyilmaz, Y. Zhang, and P. Kim, Phys. Rev. Lett. **98**, 206805 (2007).
[4] B. Özyilmaz, P. Jarillo-Herrero, D. Efetov, and P. Kim, Appl. Phys. Lett. **91**, 192107 (2007).
[5] F. Cervantes-Sodi, G. Csanyi, S. Piscanec, and A. C. Ferrari, Phys. Rev. B **77**, 165427 (2008).
[6] Z. Chen, Y.-M. Lin, M. J. Rooks, and P. Avouris, Physica E **40**, 228 (2007).
[7] A. Deshpande, W. Bao, F. Miao, C. N. Lau, and B. J. LeRoy, Phys. Rev. B **79**, 205411 (2009).
[8] J. Martin, N. Akerman, G. Ulbricht, T. Lohmann, J. Smet, K. V. Klitzing, and A. Yacoby, Nat. Phys. **4**, 144 (2008).
[9] Y. Zhang, V. W. Brar, C. Girit, A. Zettl, and M. F. Crommie, Nat. Phys. **5**, 722 (2009).
[10] J. Berezovsky, M. F. Borunda, E. J. Heller, and R. M. Westervelt, arXiv:0907.0428v2 (unpublished).
[11] E. J. H. Lee, K. Balusubramanian, R. T. Weitz, M. Burghard, and K. Kern, Nat. Nanotechnol **3**, 486 (2008).
[12] T. Mueller, F. Xia, M. Freitag, J. Tsang, and P. Avouris, Phys. Rev. B **79**, 245430 (2009).
[13] Y.-J. Yu, Y. Zhao, S. Ryu, L. E. Brus, K. S. Kim, and P. Kim, Nano Lett. **9**, 3430 (2009).
[14] C. Casiraghi, S. Pisana, K. S. Novoselov, A. K. Geim, and A. C. Ferrari, Appl. Phys. Lett. **91**, 233108 (2007).
[15] C. Stampfer, F. Molitor, D. Graf, K. Ensslin, A. Jungen, C. Hierold, and L. Wirtz, Appl. Phys. Lett. **91**, 241907 (2007).
[16] A. Das, S. Pisana, S. Piscanec, B. Chakraborty, S. K. Saha, U. V. Waghmare, R. Wang, H. R. Krishnamurthy, A. K. Geim, A. C. Ferrari, and A. K. Sood, Nat. Nanotechnol. **3**, 210 (2008).
[17] K. S. Novoselov, A. K. Geim, S. V. Morozov, D. Jiang, Y. Zhang, S. V. Dubonos, I. V. Grigorieva, and A. A. Firsov, Science **306**, 666 (2004).
[18] L. A. Ponomarenko, R. Yang, T. M. Mohiuddin, M. I. Katsnelson, K. S. Novoselov, S. V. Morozov, A. A. Zhukov, F. Schedin, E. W. Hill, and A. K. Geim, Phys. Rev. Lett. **102**, 206603 (2009).
[19] J. H. Chen, C. Jang, M. Ishigami, S. Xiao, W. G. Cullen, E. D. Williams, and M. S. Fuhrer, Solid State Commun. **149**, 1080 (2009).
[20] P. Blake, R. Wang, S. V. Morozov, F. Schedin, L. A. Ponomarenko, A. A. Zhukov, R. R. Nair, I. V. Grigorieva, K. S. Novoselov, and A. K. Geim, Solid State Commun. **149**, 1068 (2009).
[21] T. Lohmann, K. von Klitzing, and J. H. Smet, Nano Lett. **9**, 1973 (2009).
[22] H. E. Romero, N. Shen, P. Joshi, H. R. Gutierrez, S. A. Tadigadapa, J. O. Sofo, and P. C. Eklund, ACS Nano **2**, 2037 (2008).
[23] J. Moser, A. Barriero, and A. Bachtold, Appl. Phys. Lett. **91**, 163513 (2007).
[24] K. I. Bolotin, K. J. Sikes, Z. Jiang, M. Klima, G. Fudenberg, J. Hone, P. Kim, and H. L. Stormer, Solid State Commun. **146**, 351 (2008).
[25] X. Du, I. Skachko, F. Duerr, A. Luican, and E. Y. Andrei, Nature (London) **462**, 192 (2009).
[26] R. Crook, C. G. Smith, C. G. Simmons, and D. A. Ritchie, J. Phys.: Condens. Matter **12**, L167 (2000).
[27] C. Casiraghi, A. Hartschuh, E. Lidorikis, H. Qian, H. Harutyunyan, T. Gokus, K. S. Novoselov, and A. C. Ferrari, Nano Lett. **7**, 2711 (2007).
[28] A. C. Ferrari, J. C. Meyer, V. Scardaci, C. Casiraghi, M. Lazzeri, F. Mauri, S. Piscanec, D. Jiang, K. S. Novoselov, S. Roth, and A. K. Geim, Phys. Rev. Lett. **97**, 187401 (2006).
[29] D. B. Farmer, Y.-M. Lin, A. Afzali-Ardakani, and P. Avouris, Appl. Phys. Lett. **94**, 213106 (2009).
[30] S. Adam, E. H. Hwang, V. M. Galitski, and S. D. Sarma, Proc. Natl. Acad. Sci. U.S.A. **104**, 18392 (2007).
[31] E. Rossi, S. Adam, and S. D. Sarma, Phys. Rev. B **79**, 245423 (2009).
[32] M. Freitag, M. Steiner, Y. Martin, V. Perebeinos, Z. Chen, J. C. Tsang, and P. Avouris, Nano Lett. **9**, 1883 (2009).